pH-dependent aggregation behavior of a sugar-amine gemini surfactant in water: Vesicles, micelles, and monolayers of hexane-1,6-bis(hexadecyl-1 '-deoxyglucitylamine)

Bergsma, M.; Fielden, M.L.; Engberts, J.B.F.N.

Published in:
Journal of Colloid and Interface Science

DOI:
10.1006/jcis.2001.7908

Publication date:
2001

Journal of Colloid and Interface Science **243,** *491-495* (2001)
doi:10.1006/jcis.2001.7908, available online at http://www.idealibrary.com on IDEAL®

pH-Dependent Aggregation Behavior of a Sugar-Amine Gemini Surfactant in Water: Vesicles, Micelles, and Monolayers of Hexane-1,6-bis(hexadecyl-1´-deoxyglucitylamine)

Mark Bergsma, Matthew L. Fielden, and Jan B. F. N. Engberts[1]

Physical Organic Chemistry Unit, Stratingh Institute, University of Groningen, Nijenborgh 4, 9747 AG Groningen, The Netherlands

Received March 22, 2001; accepted July 24, 2001

The pH-dependent aggregation behavior of one representative of a recently described series of sugar-amine gemini surfactants has been investigated. The surface tension (g) and turbidity of hexane-1,6-bis(hexadecyl-1´-deoxyglucitylamine) drop steeply between pH 5.5 and 4.0, consistent with a vesicle-to-micelle transition. The critical micelle concentration (cmc) at low pH (3.0) was determined by surface tension measurements to be 1×10^{-3} M. This value is high, as g is at the cmc (57 mN m^{-1}). The area per headgroup (A_h) extracted from the slope of the curve of g vs concentration below the cmc is 109 Å^2. In an attempt to obtain a reasonable estimate of the headgroup area at higher pH, surface pressure vs area measurements were performed on a monolayer supported on pure water (pH 6), providing an A_h of ca. 69 Å^2. The dependence of A_h on pH is consistent with the proposed vesicle-to-micelle transition. Measurements of the gel-to-liquid crystalline phase transition using differential scanning calorimetry at a range of pHs revealed a drop in both the phase transition temperature and the transition enthalpy with decreasing pH. The pH dependence of the aggregation behavior can thus be summarized as follows: (1) pH 7.5-5.5, bilayer vesicles; (2) pH 5.5-4.0, a "drop region" where aggregate morphology is sensitive to small changes in pH; and (3) pH < 4.0, micelles.

Key Words: **vesicles; micelles; monolayer; pH-induced; phase transition; DSC; surface tension; surface pressure; microscopy.**

INTRODUCTION

Vesicle-to-micelle transitions of surfactant systems in water have been observed for a variety of amphiphiles. Most of these transitions are induced by mixing vesicle-forming surfactants with micelle-forming surfactants at different ratios (1-7) or by increasing the temperature of an ionic surfactant system resulting in a decrease of counterion binding (8). The transitions can be explained in terms of the packing parameter (9) $P = V/(a_0 l)$, where an increased headgroup area results in higher curvature and eventually in a transition to micelles (10). Dimerizing surfactant molecules via a "spacer" unit to form so-called "gemini surfactants" (11) allows further fine control of the molecular architecture and hence aggregate morphology. It was found that upon mixing two such gemini surfactants with varying spacer length, either micelles or vesicles are formed, and a vesicle-to-micelle transition has been observed (6). A pH-induced vesicle-to-micelle transition has reported by Nishikawa *et al.* (12) for a mixture of a micelle-forming surfactant and a vesicle-forming lipid. To the best of our knowledge, no single-component surfactant solution has been observed to undergo such a transition.

In a recent study on carbohydrate-based nonionic gemini surfactants, Pestman *et al.* (13) demonstrated that the aggregation state, which for conventional single-tailed surfactants is almost exclusively micellar (14), could be changed to vesicular simply by connecting the headgroups via an alkyl spacer. We have subsequently replaced the amide linking groups for amines afforded gemini surfactants with pH-titratable headgroups (15). Variation in the protonation state of these types of geminis would lead to changes in headgroup area and, as a result, in their aggregation state. These compounds have been shown to be efficient vectors for delivery of DNA to eukaryotic cells (15). Furthermore, the compounds which were most efficient for DNA delivery were also shown to undergo a vesicle-to-micelle transition in the endosomal pH range (7.4-4.0). The exact pH at which the transition occurred depends primarily, and rather strongly, on the alkyl tail length. A change of aggregation state in the endosome provides a possible mechanism for the escape of DNA via disruption of the endosomal membrane and subsequent contents release. The apparent connection between aggregation state and transfection efficiency prompted a selection of one representative compound to perform a more detailed study of the pH-dependent aggregation behavior. The present paper describes such a study for hexane-1,6-bis(hexadecyl-1´-deoxyglucitylamine) (16-6-16, Fig. 1) using a number of different techniques.

MATERIALS AND METHODS

Chemicals. The synthesis of the 16-6-16 used in this study has been described elsewhere (15).

[1] To whom correspondence should be addressed. Fax: 0031-50-363-4296. E-mail: J.B.F.N.Engberts@chem.rug.nl.

0021-9797/01 $35.00

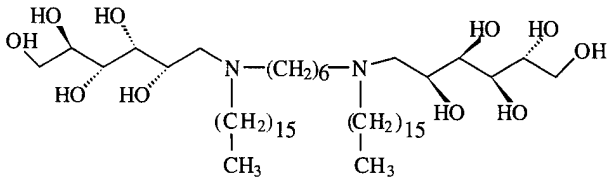

FIG. 1. Structure of gemini surfactant 16-6-16.

Differential scanning calorimetry. All DSC measurements were performed by using a differential scanning microcalorimeter (Microcal, Northampton, MA) with double-distilled water in the reference cell under N_2 (1.5 bar). The gel-to-liquid crystalline transition of the surfactant bilayers was measured by scanning between 5 and 100°C at a scan rate of 30°C h^{-1}, and employing a 2 s filter time. To check the reversibility of the transition, repeat scans were measured after slow cooling to 5°C. The baseline measurement of water versus water was subtracted from the measured plots. Enthalpies are not calculated because of minor variations in concentration of surfactant, which makes it impossible to determine enthalpies with sufficient accuracy, only allowing an examination of trends in enthalpies within an error margin of about 10%.

Drop tensiometry. Surface tension (g) measurements at 45°C on surfactant solutions were performed on a Lauda TVT-1 drop tensiometer, with a Lauda RM6 temperature controller. A surface tension value for bidistilled water of greater than 70 mN m^{-1} was taken as an internal standard before starting measurements on surfactant solutions. The concentration of the surfactant solution was 1 mg ml^{-1} and decreased slightly with decreasing pH, due to the addition of a HCl solution (0.01 or 0.1 M). The cmc measurements were performed on samples having a fixed 1:2.8 surfactant to HCl ratio at 45°C.

Light microscopy. Light microscopy pictures were obtained with an Olympus BX 60 microscope. Drops of a vesicle solution were placed on a glass slide and covered with a coverslip.

Surface pressure measurements. Surface pressure-molecular area isotherms were measured by using a Lauda Film balance (FW2). One hundred microliters of stock solution (3.02×10^{-4} M surfactant in chloroform) was carefully brought on top of the water layer between the two barriers. After a 5-min period for the chloroform to evaporate, the measurement was started. Isotherms were determined at a speed of 8.5 $Å^2$/min. The temperature of the measurements was controlled by a Neslab RTE 111 cryostat. Water for the subphase was purified by reverse osmosis and subsequent filtration through a Milli-Q purification system (16).

Preparation of vesicle solutions. Vesicles were prepared by sonication of an aqueous solution of 16-6-16 (1 mg ml^{-1}) with a Branson cell disruptor (6-15 min, 40 W pulsed) without cooling. Sonication was started after solutions were heated above the main phase transition temperature of the surfactant. It was not necessary to make films of surfactant before sonication to obtain vesicle solutions.

Turbidity measurements. Turbidity was measured at λ = 350 nm^{-1} by using a Perkin Elmer Lambda 5 spectrophotometer. Solutions of approximately 1 mg ml^{-1} surfactant were measured in a 1-mm-thick quartz cell placed in a thermostated (25°C) block. The pH of the solutions was changed by adding drops of HCl (0.01 or 0.1 M).

RESULTS AND DISCUSSION

Microscopy

Figure 2 shows an optical micrograph of a 1 mg ml^{-1} solution of hexane-1,6-bis(hexadecyl-1´-deoxyglucitylamine) (16-6-16, Fig. 1) at pH 7.5. Large vesicles are present varying in size from 0.5 mm (or smaller but not visible) to 2 mm. This micrograph was taken almost three months after the vesicle solution was prepared. The vesicular morphology was confirmed by cryo transmission electron microscopy (15). This EM picture shows smaller vesicles, which are not visible on the light microscopy pictures. Usually vesicles are believed to be metastable, which means that they tend to precipitate after some time. In our case some precipitation was observed, but this did not noticeably affect the micrograph. This type of behavior was also observed by Danino and co-workers (6). In the present case, stabilization of bilayer vesicles may result from interheadgroup hydrogen bonding. A similar micrograph was observed for freshly prepared solutions.

Surface Tension and Turbidity

Figure 3 shows the surface tension (g) as a function of pH for an aqueous solution of 16-6-16 (1 mg ml^{-1}) at 45°C. At this temperature the bilayers are in the liquid crystalline state, as indicated by differential scanning microcalorimetry (see below). The surface tension of a solution is defined as the change in surface Gibbs energy upon a change in the area of the

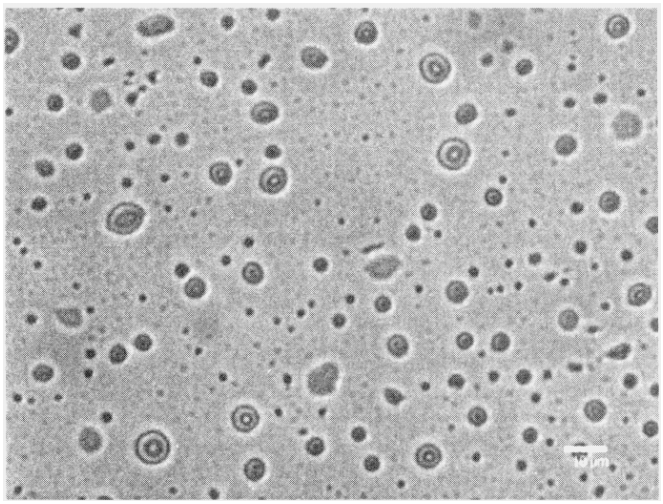

FIG. 2. Optical microscopy photo of 16-6-16. The bar represents 10 mm.

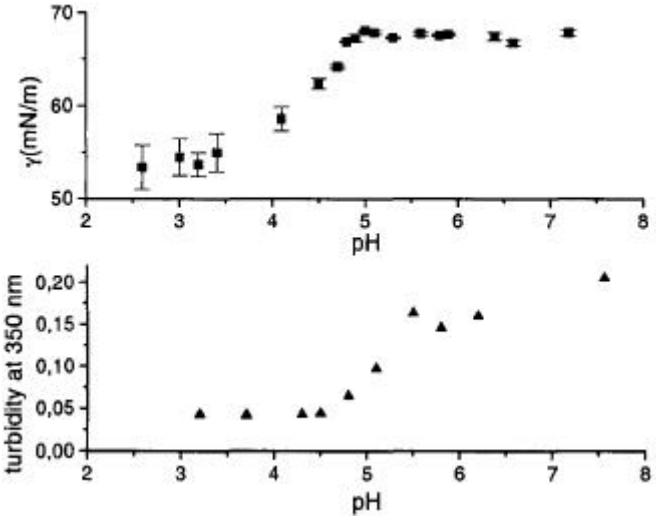

FIG. 3. Dependence of turbidity and surface tension on the pH of solutions of 16-6-16.

surface (17),

$$g = dG / ds, \qquad [1]$$

where G is the surface Gibbs energy and s is the area of the surface. The presence of surfactants in an aqueous solution lowers the surface tension as a result of the accumulation of surfactant at the air-water interface. This phenomenon is described by the Gibbs isotherm

$$\Gamma = -\left(\frac{\partial g}{\partial c}\right)\frac{c}{RT}, \qquad [2]$$

in which Γ is the surface excess (mol m^{-2}), c is the surfactant concentration (M), R is the gas constant, and T is the absolute temperature. From this isotherm it is apparent that the surface tension is lowered as more surfactant accumulates at the air-water interface, and hence, the surface tension will decrease as the concentration of free surfactant is increased. At high pH the surface tension approaches the value for the surface tension of pure water (ca. 69 mN/m at 45°C) (18), whereas at low pH surface tension values are much lower, indicating a largely increased solubility, and hence larger availability of the monomers for adsorption at the air-water interface upon decreasing pH. Figure 4 shows a plot of surface tension versus log c. A break in this plot is observed at 1 mM, just below the concentration of surfactant used in all other experiments described in the present study. At this concentration the cmc (critical micelle concentration) is reached. The shallow minimum observed in the plot of Fig. 4 may be caused by the presence of monoprotonated gemini or alternatively by a small amount of surface active monomeric impurity which could not completely be removed. We note that g_{cmc} has a remarkably high value and that the cmc also high compared to that of comparable gemini surfactants with quaternary ammonium headgroups but without sugar groups (19). In fact, the cmc is comparable with that of $C_{16}H_{33}N^{+}(CH_3)_3Br^{-}$ (1 mM) (20). High cmcs have also been observed for other gemini surfactants. Rosen and Menger (11, 21, 22) ascribe this behavior to the formation of premicellar aggregates (dimers, trimers, oligomers), which are assumed not to be surface active. Impairment of adsorption at the air-water interface could also play a role. Instead of a simple equilibrium between two states, a more complicated equilibrium between several aggregation states may be involved. From the slope of the graph of surface tension versus log c (c < cmc) an estimate of the area occupied by one molecule at the air-water interface can be made (17). Equation [2] can also be written as

$$\Gamma = \frac{1}{nRT}\frac{dg}{d\ln c} = \frac{1}{2.303nRT}\frac{dg}{d\log c}, \qquad [3]$$

where n is the fraction of bound counterions. From the obtained surface excess (Γ), the area per molecule can be estimated

$$a = \frac{1}{\Gamma N_a}, \qquad [4]$$

in which N_a is Avogadro's number. Estimating n is problematic in this case due to the unknown ionization state. However, in the presence of a swamping amount of electrolyte, this value can be taken as 1 (full counterion binding). For a 1 : 1 ratio of ionic surfactant to counterion, this value is taken as 2 and for gemini surfactants (1 : 2 ratio) n has often been taken as 3 (23-25). Sometimes n = 2 has been used for gemini surfactants under the assumption that one of the headgroups is bound by a counterion (19). In our solutions 1 equivalent excess of HCl is present, and almost all of the surfactants are assumed to be protonated; therefore we can set n = 2. Due to the above-mentioned uncertainties the obtained area per molecule of 109 $Å^2$ should be taken as an

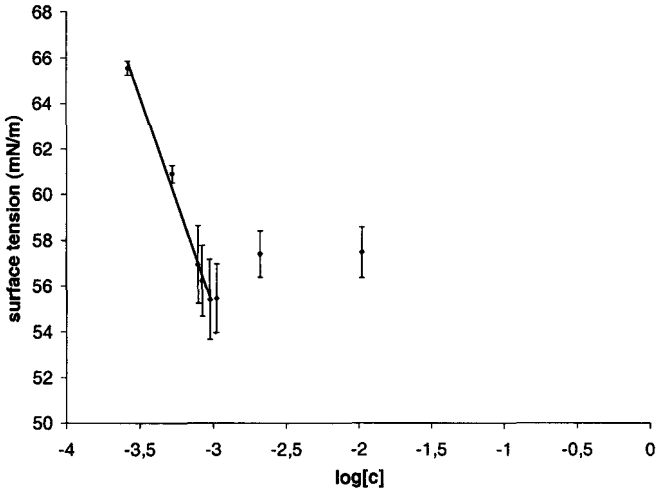

FIG. 4. Surface tension of solutions of 16-6-16 with 3 equivalents of HCl as a function of concentration.

approximate value. The relatively large errors in g (Figs. 3 and 4) are caused by a systematic decrease in surface tension during a series of measurements. A series of 4 times 2 surface tension measurements has been performed on the drop tensiometer to obtain one surface tension value. Within this series the surface tension value decreases systematically, which is something we cannot explain. Repeat measurements on the same sample show the same pattern. The errors are larger in the drop region of the graph.

Figure 3 displays a graph of the turbidity (at 350 nm) against pH for the same solutions. It is possible to distinguish three regions in this graph. Above pH 5.5 the solutions have a nearly constant turbidity, except for the turbidity of the solution at pH 7.5. At pH 7.5 the turbidity is much higher (0.8) and the solution appears milky instead of clear blueish. In this solution precipitation was observed. At pH 5.5 the turbidity starts to drop, reaching a plateau value at pH 4.5. The solutions with a pH lower than 4.5 are clear to the eye and typical for a micellar solution.

The drop in surface tension starts at a lower pH (5.0) than the drop in turbidity (pH 5.5) and plateaus at a lower pH (4.0 vs 4.5 for turbidity). This means that the process of solubilization of monomers starts at a lower pH than the disappearance of the largest aggregates. It may well be that the increased number of protonated surfactants increases the curvature strain and that this causes the break-up of the largest aggregates.

Differential Scanning Calorimetry

Figure 5 shows gel-to-liquid crystalline phase transition temperatures of bilayers of 16-6-16 at different pHs as measured by DSC (26). As the pH falls below pH 5, the transition temperature decreases rapidly from about 40 to 28°C. This indicates that the bilayer becomes less tightly packed as the pH is decreased, which can be attributed to the increased headgroup size due to protonation of the nitrogen atoms. At pH < 4.3 a transition is no longer measurable. Figure 6 shows that the size of the peaks

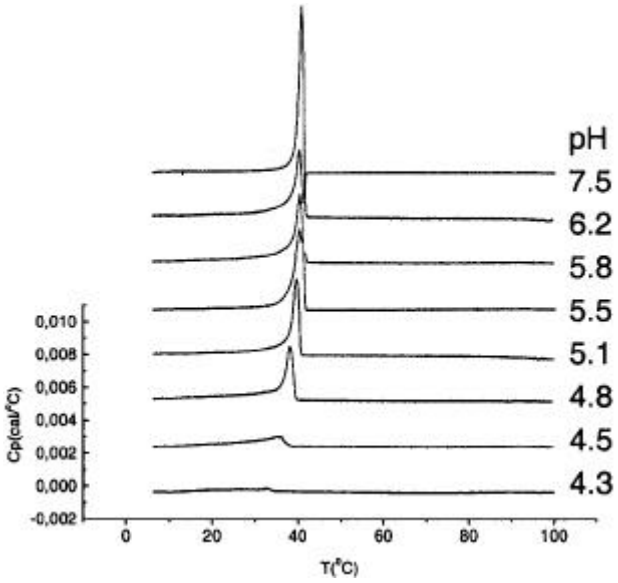

FIG. 6. DSC thermograms of 16-6-16 at different pHs.

is also decreasing steeply below pH 5. Below pH 4.3 almost no surfactant molecules are assembled in bilayers, and therefore, no gel-to-liquid crystalline transitions of bilayers are observed (27).

Langmuir Films

Figure 7 is a lateral pressure/area per molecule isotherm of a monolayer of 16-6-16 at 21°C. Surface pressure (p) is defined as the reduction in surface tension of a fluid as surfactant is added,

$$p = g_0 - g\,, \qquad [5]$$

where g_0 is the surface tension of water and g is the surface tension of water with the surfactant monolayer. The area

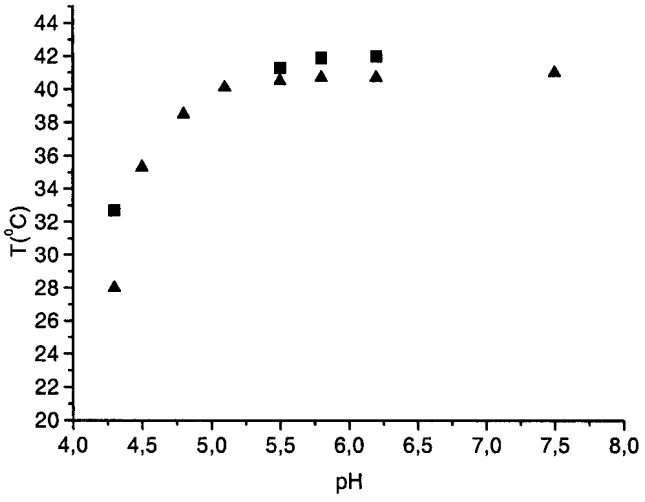

FIG. 5. Dependence of T_m of 16-6-16 as a function of pH: (▲) T_m1 and (■) T_m2.

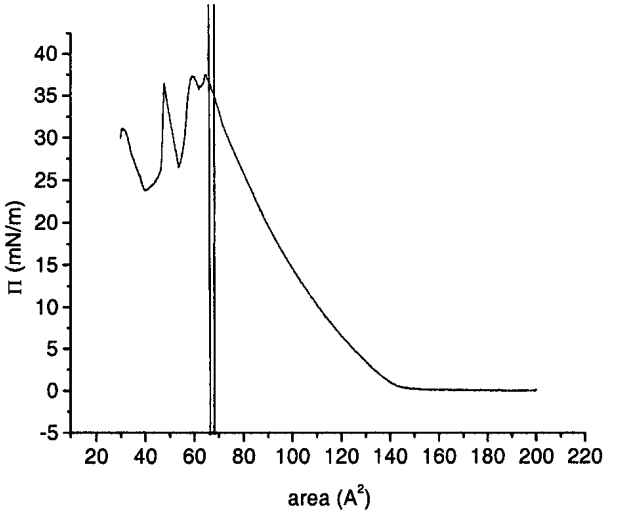

FIG. 7. Langmuir isotherm of 16-6-16 at 22°C. The vertical lines give an indication of the expected headgroup area for a bilayer of the same compound.

per molecule in between the bars is the expected area occupied by a molecule in a bilayer as is theoretically and experimentally derived from comparison of monolayers with bilayers (ca. 35 mN/m) (28), which in the case of 16-6-16 is around 69 Å^2. The isotherm does not change upon increasing the temperature to 29°C (isotherms not shown). Recalling that the estimated area per molecule as revealed by the surface tension measurements at low pH is 109 Å^2, it appears that the size of the headgroup is increased upon lowering the pH. This is anticipated since the repulsion between gemini headgroups is increased upon protonation, which is the cause of the change in aggregation morphology.

CONCLUSION

On the basis of the above measurements it is now possible to provide a picture of the pH-induced vesicle-to-micelle transition. Starting at high pH, vesicles are present as shown by optical microscopy and DSC. At pH 5.5 the largest vesicles start to break up as shown by the decrease in turbidity. From pH 5 the reduced surface tension indicates an increased monomer solubility. Plateau values for turbidity and surface tension are reached at pH 4.5 and pH 4, respectively, DSC measurements show a decrease in T_m due to increased headgroup repulsions as the pH is lowered in the drop region. A micellar region is observed below pH 4. The CMC (1 mM) is high as is the surface tension at the CMC (57 mN m^{-1}), As the pH is lowered from 7.5 to 4.0, the effective size of the headgroups is increased from approximately 69 to 109 Å^2. Although both numbers are estimates, they clearly illustrate the expected trend.

ACKNOWLEDGMENTS

The Department of Biophysical Chemistry (Professor G. T. Robilard and Professor B. Poolman) is acknowledged for use of the DSC equipment. We thank Professor A. J. Schouten for the use of the film balance. M.B. thanks Rudi Oldenzijl and Gerard Nijboer for their help in performing Langmuir measurements. M.F. acknowledges the European Union for financial support (Framework IV-European Network on Gemini Surfactants, ENGEMS).

REFERENCES

1. Brinkmann, U., Neumann, E., and Robinson, B. H., *J. Chem. Soc., Faraday Trans.* **94,** 1281-1285 (1998).
2. Cantu, L., Corti, M., and Del Favero, E., *J. Mol. Liq.* **71,** 151-161 (1997).
3. de la Maza, A., and Parra, J. L., *Biochem. J.* **303,** 907-914 (1994).
4. de la Maza, A., and Parra, J. L., *Langmuir* **11,** 2435-2441 (1995).
5. Uchegbu, I. F., Bouwstra, J. A., and Florence, A. T., *J. Phys. Chem.* **96,** 10548-10553 (1992).
6. Danino, D., Talmon, Y., and Zana, R., *J. Colloid Interface Sci.* **185,** 84-93 (1997).
7. Carion-Taravella, B., Chopineau, J., Ollivon, M., and Lesieur, S., *Langmuir* **14,** 3767-3777 (1998).
8. Buwalda, R. T., Stuart, M. C., and Engberts, J. B. F. N., *Langmuir* **16,** 6780-6786 (2000).
9. Israelachvili, J. N., "Intermolecular and Surface Forces." Academic Press, London, 1994.
10. Menon, S. V. G., Manohar, C., and Lequeux, F., *Chem. Phys. Lett.* **263,** 727-732 (1996).
11. Menger, F. M., and Littau, C. A., *J. Am. Chem. Soc.* **113,** 1451-1452 (1991).
12. Nishikawa, N., Arai, M., Ono, M., and Itoh, I., *Langmuir* **11,** 3633-3635 (1995).
13. Pestman, J. M., Kevelam, J., Blandamer, M. J., van Doren, H. A., Kellogg, R. M., and Engberts, J. B. F. N., *Langmuir* **15,** 2009-2014 (1999).
14. Blunk, D., Praefcke, K., and Vill, V., *in* "Handbook of Liquid Crystals" (D. Demus, J. W. Goodby, G. W. Gray, H. W. Spiess, and V. Vill, Eds.), p. 305-340. Wiley-VCH, Weinheim, 1998.
15. Fielden, M. L., Perrin, C., Kremer, A., Bergsma, M., Stuart, M. C., Camilleri, P., and Engberts, J. B. F. N., *Eur. J. Biochem.* **268,** 1269-1279 (2001).
16. Hagting, J., Ph.D. thesis, p. 26. University of Groningen, 1999.
17. Rosen, M. J., "Surfactants and Interfacial Phenomena." Wiley-Interscience, New York, 1978.
18. "CRC Handbook of Chemistry and Physiscs," 80th ed., CRC Press, Boca Raton, FL, 1999.
19. Devinsky, F., Lacko, I., Bittererova, F., and Tomeckova, L., *J. Colloid Interface Sci.* **114,** 314-322 (1986).
20. Dam, T., Engberts, J. B. F. N., Karthäuser, J., Karaborni, S., and Van Os, N. M., *Colloids Surf. A* **118,** 41-49 (1996).
21. Song, L. D., and Rosen, M. J., *Langmuir* **12,** 1149-1153 (1996).
22. Menger, F. M., and Littau, C. A., *J. Am. Chem. Soc.* **115,** 10083-10090 (1993).
23. Alami, E., Beinert, G., Marie, P., and Zana, R., *Langmuir* **9,** 1465-1467 (1993).
24. Devinsky, F., Masarova, L, and Lacko, I., *J. Colloid Interface Sci.* **105,** 235-239 (1985).
25. Abid, S. K., Hamid, S. M., and Sherrington, D. C., *J. Colloid Interface Sci.* **120,** 245-255 (1987).
26. Jaeger, D. A., and Brown, E. L. G., *Langmuir* **12,** 1976-1980 (1996).
27. Solutions of micelles can also display endothermic effects: Blandamer, M. J., Briggs, B., Burgess, J., Butt, M. D., Brown, H. R., Cullis, P. M., and Engberts, J. B. F. N., *J. Colloid Interface Sci.* **150,** 285-290 (1992); Blandamer, M. J., Briggs, B., Burgess, J., Cullis, P. M., and Eaton, G., *J. Chem. Soc., Faraday Trans.* **87,** 1169-1175 (1991).
28. Marsh, D., *Biochim. Biophys. Acta* **1286,** 183-223 (1996).